High Temp. Mater. Proc., Vol. **30** (2011), pp. 289–296 DOI 10.1515/HTMP.2011.047

Fiber-reinforced Yttria Partially Stabilized Zirconia Thermal Barrier Coatings Processed by Sol-gel Method

Junguo Gao,[1] **Yedong He**[1] **and Wei Gao**[2,*]

[1] Beijing Key Laboratory for Corrosion, Erosion and Surface Technology, University of Science and Technology Beijing, Beijing, P.R. China

[2] Department of Chemicals and Materials Engineering, The University of Auckland, Auckland, New Zealand

Abstract. A novel fiber-reinforced 6 wt% yttria partially stabilized zirconia (YPSZ) thermal barrier coating (TBC) has been produced by sol-gel process The coating showed superior high-temperature properties compared with the traditional sol-gel TBCs Hollow Al_2O_3-10 mol% ZrO_2 fibers were used to reinforce the sol-gel TBCs. SEM and XRD results showed that the coatings obtained were dense, uniform and crack-free with the main phase of yttria stabilized t-ZrO_2. High-temperature cyclic oxidation test at 1000°C for 200 h and thermal insulation test were also performed to investigate the oxidation resistance and thermal insulation property of the coating. It revealed that the addition of hollow Al_2O_3-ZrO_2 fibers not only enhanced the mechanical property but also created high porosity in the coatings, which finally improved the oxidation and spallation resistance as well as the thermal insulation of such coatings.

Keywords. Fiber-reinforced thermal barrier coatings, sol-gel; hollow Al_2O_3-ZrO_2 fibers, oxidation and scale spallation resistance, thermal insulation property.

PACS®(2010). 81.65.Kn.

1 Introduction

Thermal barrier coatings (TBCs) are widely used on the hot section components of aircraft engines, marine propulsion and industrial gas turbines to reduce operating temperatures, which can promote overall engine efficiency [1]. TBCs usually consist of a MCrAlY (where M = Ni, Co or both) bond coat, a ceramic (usually yttria partially stabilized zirconia) top coat, and a thermally grown oxide (TGO). The TGO is formed at the interface between the bond coat and the top coat via oxidation of the bond coat during the operation of the gas turbine. At an industrial scale, two dry-route processes, plasma spraying (PS) and electron beam physical vapor deposition (EB-PVD), are used to fabricate TBCs. And the TBCs fabricated by these two methods have different microstructures [2]: lamellar microstructure consisting of splats superposition for PS coatings with thermal conductivity in the range from 0.7 to 0.9 $W\,m^{-1}\,K^{-1}$ [3] and column-like microstructure for EB-PVD coatings with good mechanical performances. In the second case, however, the perpendicular growth of the columns makes the twice thermal conductivity as the PS coating.

TBCs prepared by the above two methods are directional and often require high equipment investment and complicated operation. Recently, a new sol-gel route has been developed to prepare thermal barrier coatings [2, 4–6]. It is a versatile process that is able to produce either thin ceramic coatings or thick deposition layers. The main advantage of this method is that it can decrease the crystallization temperature to a much lower point than the conventional processes. Furthermore, the sol-gel process is a nondirectional deposition technique, which is very different from the PS or EBPVD methods. And the non-oriented microstructure is expected to possess satisfactory thermo-mechanical behavior when the TBC is cyclically oxidized [7]. However, cracking or even spallation during sintering or usage is one of the main problems for sol-gel processed coatings which largely limit its applications.

In this paper, a new method, fiber-reinforced thermal barrier coatings, is proposed base on sol-gel process. The aim of this work is attempting to improve the mechanical and thermal insulation properties of thermal barrier coatings by means of introducing hollow Al_2O_3-ZrO_2 fibers.

2 Experimental Procedures

MCrAlY alloy with the nominal composition of Ni-32Co-20Cr-8Al-0.5Y has been chosen as the substrate. All surfaces of the specimens were ground to #1500 abrasive paper (Ra = 3.14 μm) before coated, followed by ultrasonic cleaning with ethanol and deionized water.

A measured amount of zirconium nitrate and yttrium nitrate were dissolved in deionized water to obtain 0.1 mol/L

Corresponding author: Wei Gao, Department of Chemicals and Materials Engineering, The University of Auckland, Auckland, New Zealand; E-mail: w.gao@auckland.ac.nz.

Received: November 8, 2010. Accepted: April 15, 2011.

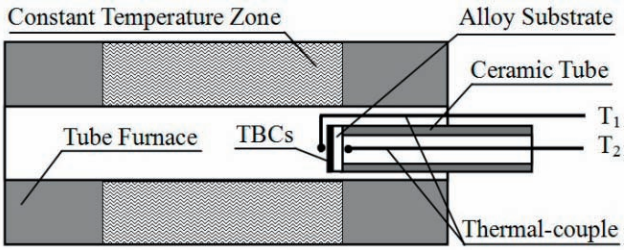

Figure 1. Schematic illustration of thermal insulation testing set-up.

solution. Citric acid (CA) was subsequently added to the solution, followed by dropwise addition of $NH_3 \cdot H_2O$ until pH equals to 7. Then a small amount of ethylene glycol (EG) was added to the solution, and the molar ratio of Zr^{4+} : CA : EG was 1 : 1 : 20. All reagents used in this work were provided by Beijing Chemical Reagents Company. After that, the solution was added with YPSZ (ZrO_2-6 wt% Y_2O_3) powder of 0.5 μm mean size (Hot Spraying Material Ltd., China) and Al_2O_3-ZrO_2 fibers to make a composite slurry. The molar ratio of ZrO_2 powder/ZrO_2 in the sol and Al_2O_3-ZrO_2 fibers/total ZrO_2 were 7/1 and 1/9, respectively.

The hollow Al_2O_3–ZrO_2 fibers were fabricated by immersion method as reported in a previous paper [8] Cotton fibers were used as template and aluminum nitrate solution (with 10 wt% zirconia nitrate) was used as immersion solution. After immersed, dried and sintered at 1200°C, the hollow ceramic fibers were finally obtained. The slurry was then coated onto the MCrAlY substrate. After dried at 80°C for 15 min and sintered at 600°C under a pressure of 9 MPa, the green coatings were then microwave sintered at the measured temperature of 1000°C for 20 min to obtain the final fiber-reinforced TBCs. The microwave frequency was 2450 MHz and the average power of the microwave furnace was approximately 2 KW. And the TBCs without fiber reinforcement were prepared in the same way.

Cyclic oxidation test was conducted in a tube furnace at 1000°C for 200 h. After every 10 h exposure, specimens were taken out and cooled in air for 20 min. The mass gain and scale spallation mass were weighed using an analytical balance with a resolution of ±0.1 mg. The thermal insulation test was performed by a device shown in Figure 1. The outside (T_1) and inside (T_2) temperatures were measured by two thermal couples.

The surface and cross-section morphologies of specimens were observed by a field emission SEM (SUPRA 55, ZEISS, Germany) equipped with an energy dispersive spectrometer (EDS). Phase identifications were conducted by X-ray diffraction (CuKα, $\lambda = 0.15406$ nm, step wise of 0.02°, continuous scanning).

3 Results and Discussion

3.1 Microstructures and Phase Compositions

The surface and cross-section morphologies of fiber-reinforced thermal barrier coatings after microwave sintering are shown in Figure 2. It can be seen that the coatings are dense and crack-free, and the fiber morphology can be observed under a higher magnification. The cross-section photographs (Figure 2(c) and Figure 2(d)) indicate that the as-prepared fiber-reinforced TBCs with a thickness of about 300 μm have a good adherence to the alloy substrate. The fibers can be also found to be inlaid tightly with the YPSZ matrix.

Figure 3 shows the XRD spectra of fiber-reinforced YPSZ thermal barrier coatings. After the microwave sintering at 1000°C, yttria stabilized tetragonal zirconia (t-ZrO_2) can be identified as the main phase. Some peaks of α-Al_2O_3 can also be seen due to the addition of Al_2O_3-ZrO_2 fibers.

The influences of fiber content on the morphologies of coatings are also investigated. As shown in Figure 4, the surface morphologies of coatings change gradually with the variation of fiber content. Among these, TBCs with the fiber content of 10 wt% showed the best reinforcement by avoiding the formation of cracks. When the fiber content increases to 20 wt%, the coating becomes not dense due to the hollow structures of the fibers added, indicating that 10% perhaps is the optimum fiber content for the best reinforcement.

3.2 High-temperature Cyclic Oxidation Kinetics

Figure 5 gives the oxidation kinetic curves of specimens with different TBCs at 1000°C for 200 h. It shows that the substrates coated with thermal barrier coatings exhibit better oxidation resistance than the blank sample due to the temperature decrease through coatings (Figure 5(a)). And the fiber-reinforced TBCs show a better oxidation resistance than TBCs without fibers, which can be seen from the scale spallation behavior. From the spallation curves in Figure 5(b), it can be seen that thermal barrier coating without fibers shows a severe spallation during cyclic oxidation. While the blank sample and fiber-reinforced TBCs exhibit almost no spallation after oxidation for 200 h. It can also be seen that the addition of fibers improves the high-temperature mechanical properties of TBCs significantly.

Surface morphologies of specimens after cyclic oxidation at 1000°C for 200 h are presented in Figure 6. It shows that the surface of blank alloy sample becomes non-uniform after oxidation with needle-shaped θ-Al_2O_3 found under a higher magnification. Comparing the oxidation surfaces of TBCs with and without fiber reinforcement, it can be seen that large cracks appear on the surface of TBCs specimen.

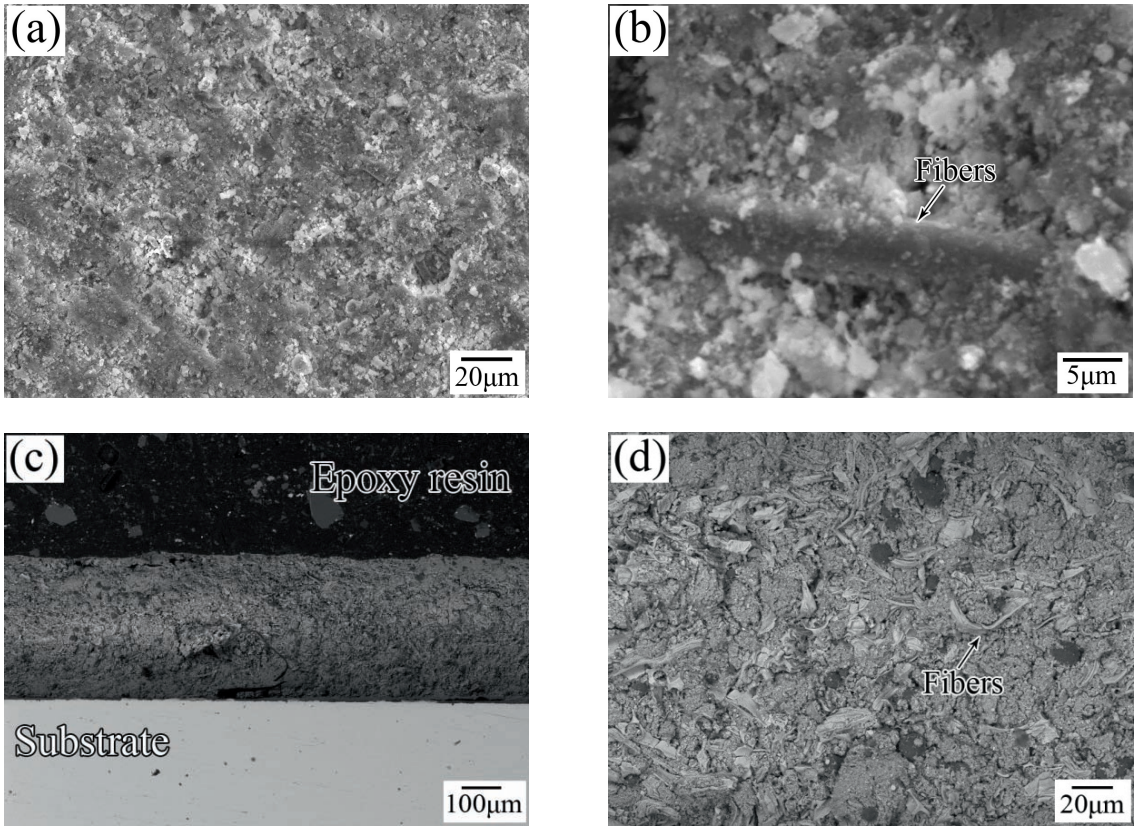

Figure 2. Surface (a, b) and cross-section (c, d) morphologies of fiber-reinforced TBCs.

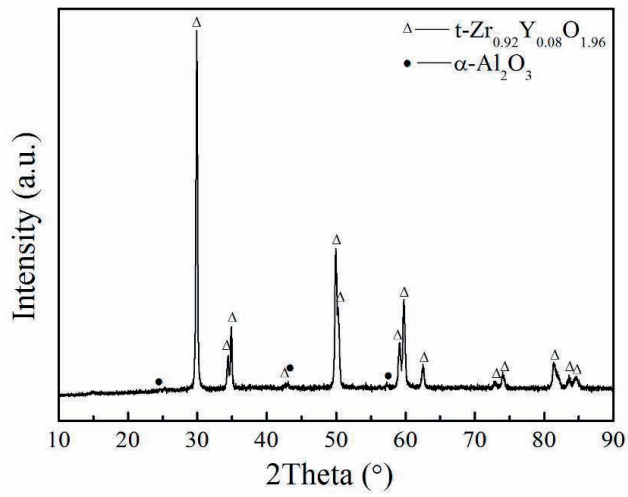

Figure 3. XRD spectra of fiber-reinforced thermal barrier coatings.

By contrast, there are only micro-sized cracks uniformly distributed on the surface of fiber-reinforced TBCs after oxidation.

Comparing the cross-section morphologies of specimens after cyclic oxidation in Figure 7, it can be found that the thermally grown oxide (TGO) of blank sample is not so uniform and continuous. Internal oxidation took place at some weak places of TGO. The same situation also appears near the TGO of TBCs specimen as marked in the micrographs. However, the TGO of fiber-reinforced TBCs specimen is comparatively uniform and continuous. Furthermore, obvious and continuous cracks formed in the vicinity of the coating/TGO interface for the TBCs specimen. For the fiber-reinforced TBCs specimen, small cracks can also be seen but they are not continuous.

Figure 8 and Figure 9 show the element distribution of TBCs and fiber-reinforced TBCs after oxidation at 1000°C for 200 h. These photographs show the cracks generated near the coatings/TGO interface It can also be seen from Figure 7 that TGO is mainly composed of Al and O and the TGO of fiber-reinforced TBCs is much uniform and continuous than that of TBCs. Moreover, the distribution of Al_2O_3-ZrO_2 fibers can be observed by element Al.

It is known that the major limitation of development and application of ceramic coatings lies in their poor fracture toughness. The coating properties may be enhanced by adding a second phase material, such as ceramic fibers or whiskers which are incorporated into the coating structure [9]. This method of composite materials has the potential of improving the fracture toughness of ceramics by mech-

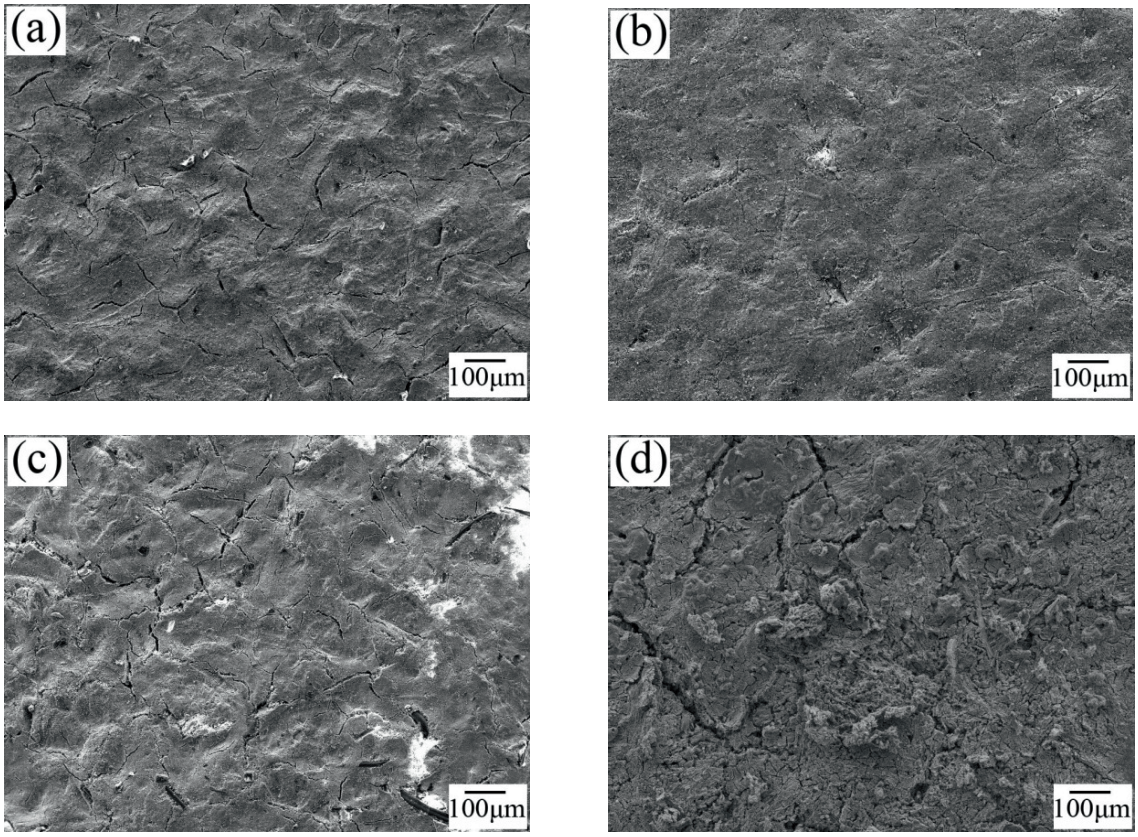

Figure 4. Surface morphologies of fiber-reinforced thermal barrier coatings with different fiber content: (a) 5 wt%, (b) 10 wt%, (c) 15 wt%, and (d) 20 wt%.

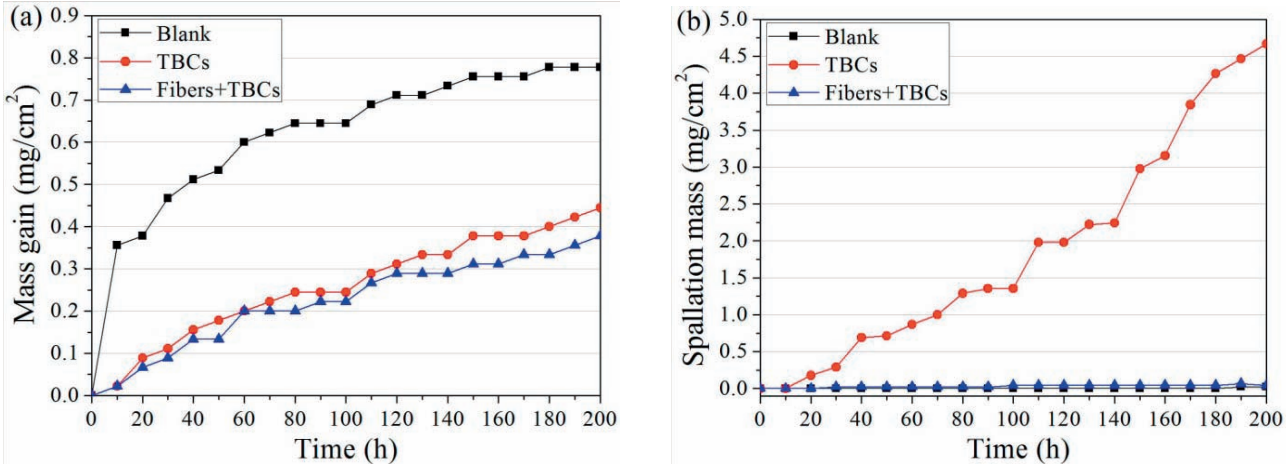

Figure 5. Oxidation kinetic curves of specimens with different thermal barrier coatings at 1000°C for 200 h: (a) mass gain versus time, and (b) spallation mass versus time.

anisms of fiber breakage, fiber pullout, fiber–matrix interface delamination and matrix fracture, etc. [10]. The influence of defects on the structural integrity of fiber-reinforced materials was studied by a number of researchers [11–13]. In particular, the flaw or crack bridging in unidirectional fiber-reinforced composites was discussed; and the model of crack bridging in composite materials was presented [14–16].

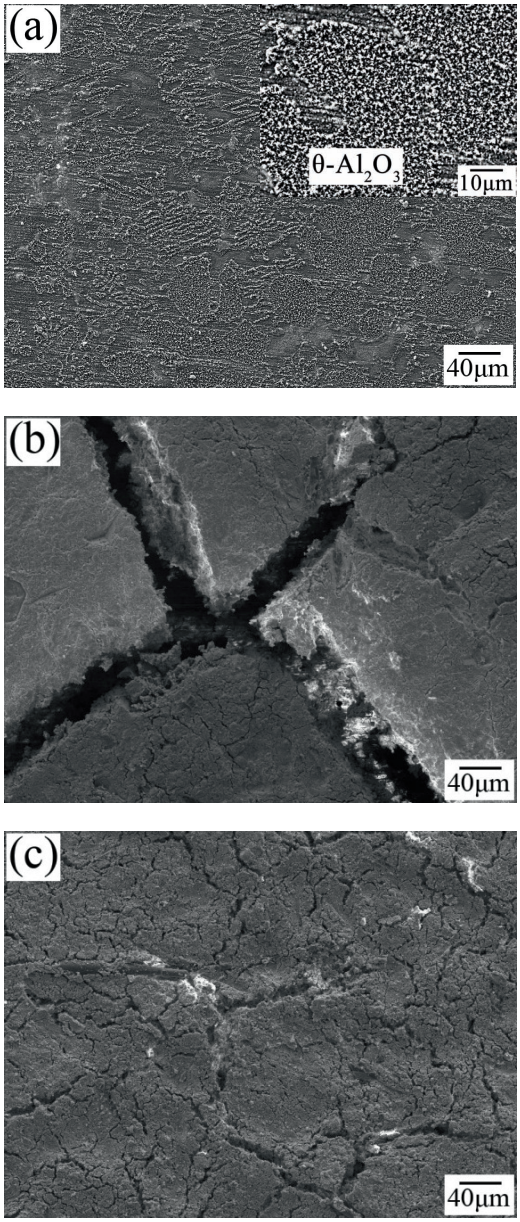

Figure 6. Surface morphologies of specimens after oxidation at 1000°C for 200 h: (a) blank alloy, (b) TBCs, and (c) fiber-reinforced TBCs.

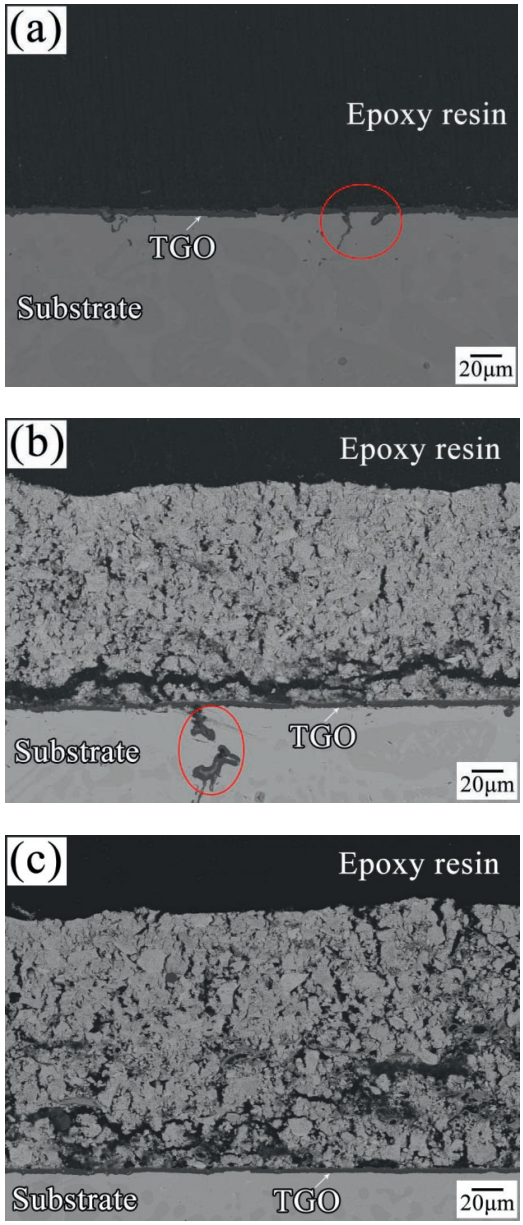

Figure 7. Cross-section morphologies of specimens after oxidation at 1000°C for 200 h: (a) blank alloy, (b) TBCs, and (c) fiber-reinforced TBCs.

In our fiber-reinforced coating system, fiber breakage and crack bridging are considered to be the main factors to improve the fracture toughness of TBCs by means of energy consumption mechanisms. Figure 10 shows the schematic model of crack bridging in unidirectional fiber-reinforced materials which is supposed to play an important role in our fiber-reinforced system. Crack bridging is a crack tail effect which means that the closure stresses can be generated on the two surfaces linked by fibers near the end of crack It can suppress the propagation of cracks and finally improve the fracture toughness of the coating.

3.3 Thermal Insulation Property

Figure 11 presents the results of thermal insulation test of different specimens under various temperatures. Comparing the inside temperature of different specimens it can be found that the fiber-reinforced TBCs have a better thermal insulation property than TBCs, which can be attribute to the increase of porosity in the coating due to the hollow structures of fibers. It is reasonable that the porosity in the coatings favors insulation property [17, 18]. It can also be seen that the insulation ability increases with increasing test temperature.

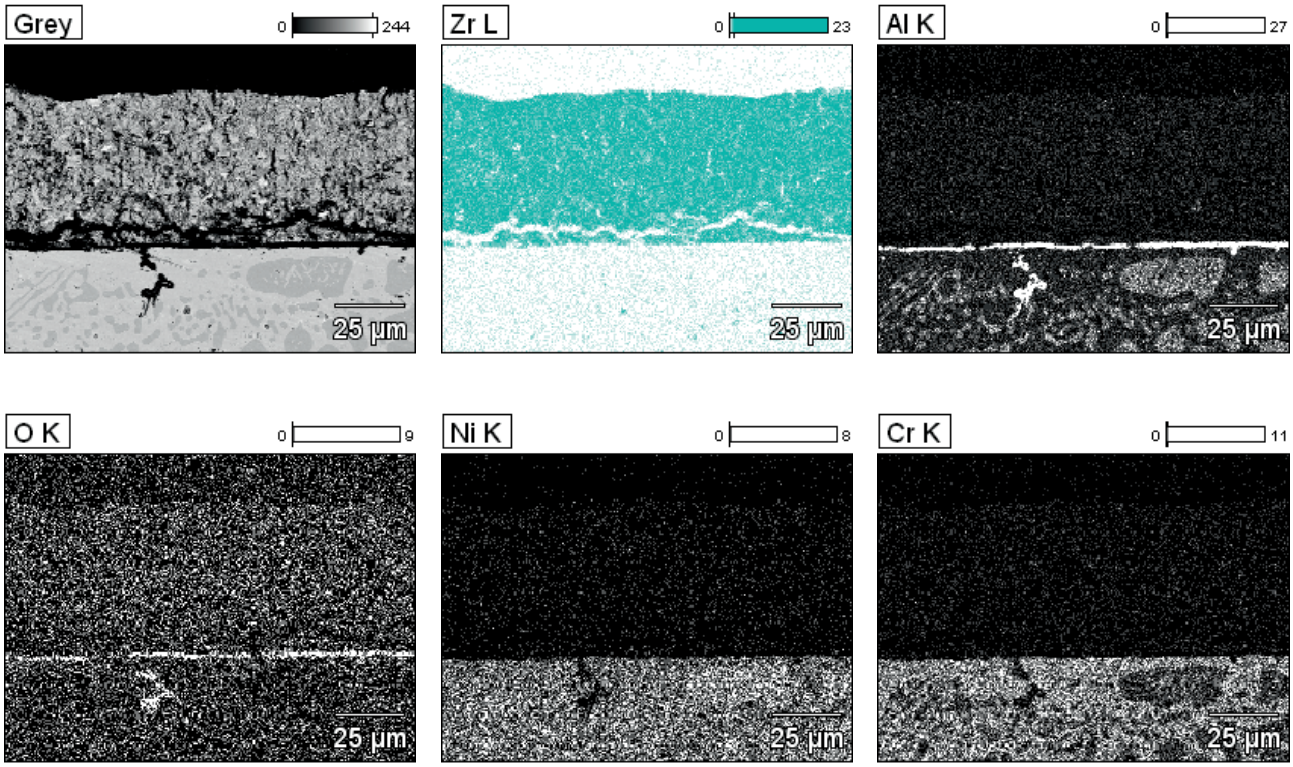

Figure 8. Element distribution of TBCs after oxidation at 1000°C for 200 h.

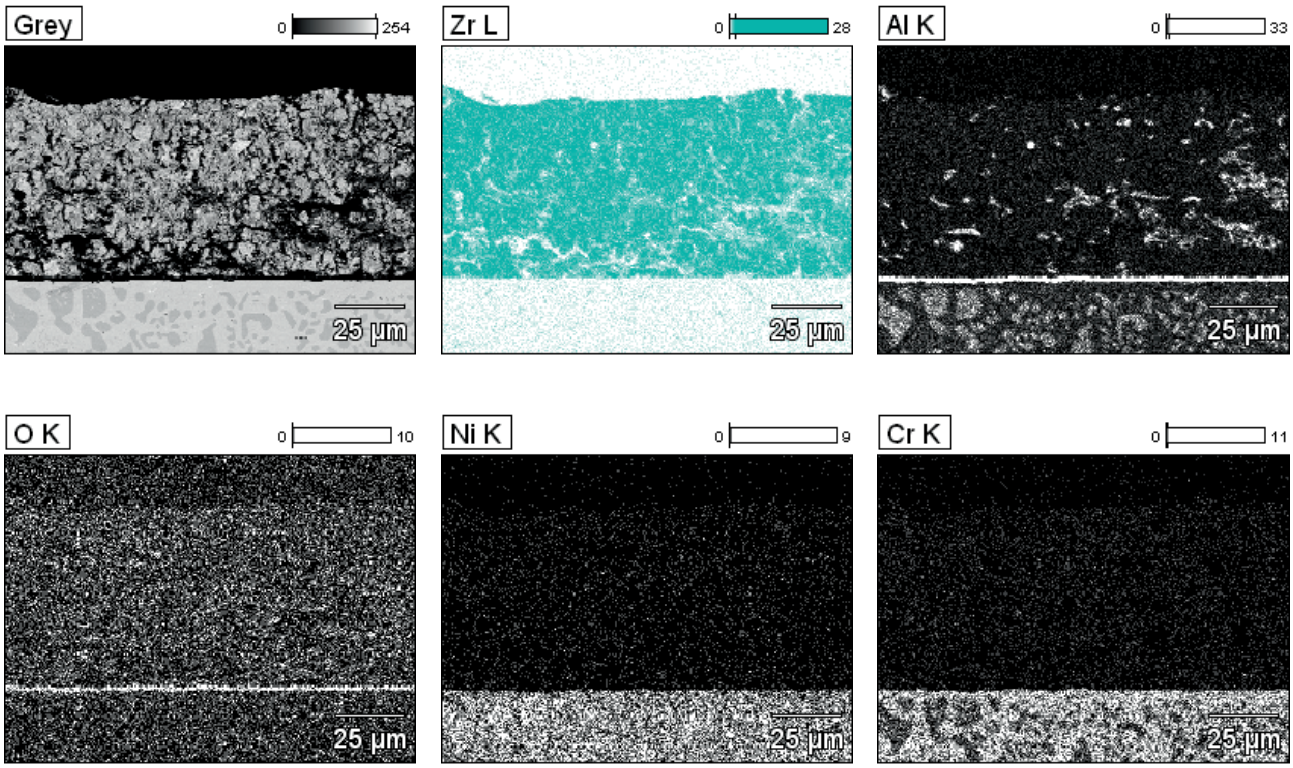

Figure 9. Element distribution of fiber-reinforced TBCs after oxidation at 1000°C for 200 h.

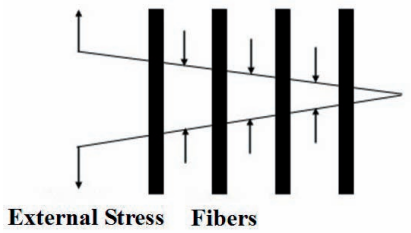

Figure 10. Crack bridging model of fibers or whiskers in fiber/whisker reinforced materials.

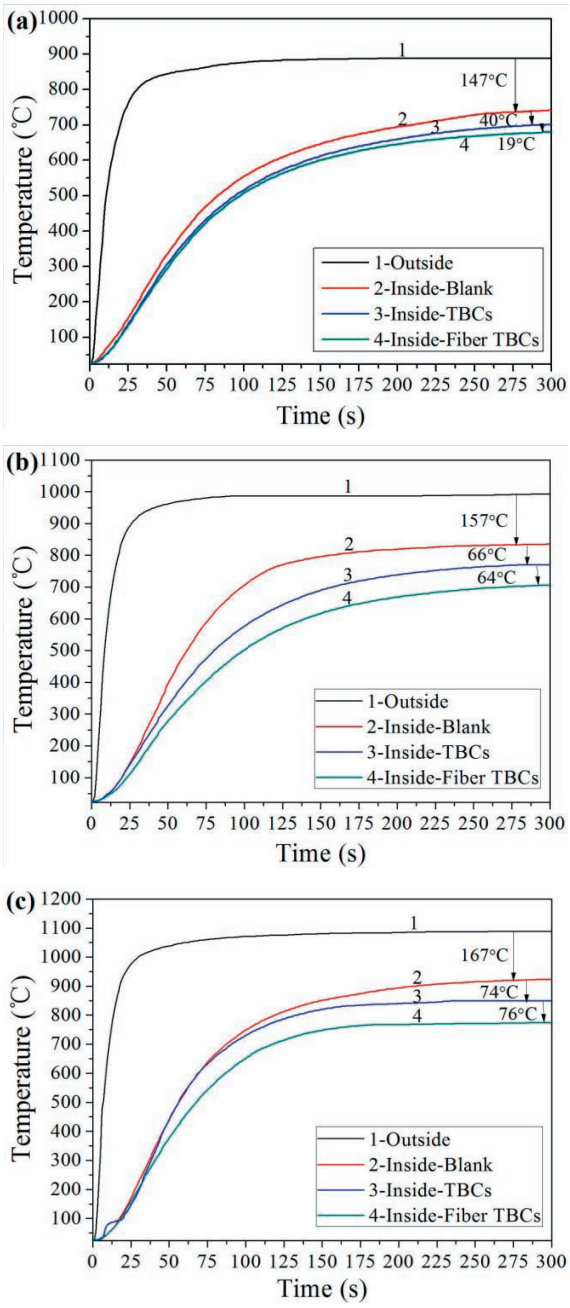

Figure 11. Outside and inside temperatures of different coatings when the outside temperature at: (a) 900°C, (b) 1000°C, and (c) 1100 °C.

4 Conclusions

Sol-gel process is a promising method to fabricate thermal barrier coatings. Compared with other methods, it has advantages of nondirectional deposition, versatility and low sintering temperature. Nevertheless, the sol-gel coatings still need improvement on their cracking and spallation resistance and thermal insulation property. From this research we propose that the addition of hollow ceramic fibers can enhance the mechanical property and create porosity of the coatings, which in turn improve the oxidation and spallation resistance as well as the thermal insulation property of TBCs With in-depth study of sol-gel fiber-reinforced TBC, it may become a useful route for either manufacturing or repairing thermal barrier coatings.

Acknowledgments

This work has been financially supported by Chinese National Natural Science Foundation Grant NO 50771021.

References

[1] R. A. Miller, Current status of thermal barrier coatings – An overview, *Surf. Coat. Technol.* **30** (1987), 1.

[2] C. Viazzi, J. P. Bonino and F. Ansart, Synthesis by sol-gel route and characterization of yttria stabilized zirconia coatings for thermal barrier applications, *Surf. Coat. Technol.* **201** (2006), 3889.

[3] W. Y. Lee, D. P. Stinton, C. C. Berdt, F. E. Erdogan and Y. D. Lee, Concept of functionally graded materials for advanced thermal barrier coating applications, *J. Am. Ceram. Soc.* **79** (1996), 3003.

[4] C. Viazzi, A. Deboni, J. Z. Ferreira, J. P. Bonino and F. Ansart, Synthesis by sol-gel route and characterization of yttria stabilized zirconium coatings for thermal barrier applications, *Solid State Sci.* **8** (2006), 1023.

[5] M. Gaudon, C. Laberty-Robert, F. Ansart and P. Stevens, Thick YSZ films prepared via a modified sol-gel route: Thickness control (8–80 µm), *J. Eur. Ceram. Soc.* **26** (2006), 3153.

[6] C. Ren, Y. D. He and D. R. Wang, Al_2O_3/YSZ composite coatings prepared by a novel sol-gel process and their high-temperature oxidation resistance , *Oxid. Met.* **74** (2010), 275.

[7] J. Sniezewski, Y. LeMaoult, P. Lours, L. Pin, V. M. Bekale, D. Monceau, D. Oquab, J. Fenech, F. Ansart and J. P. Bonino, Sol-gel thermal barrier coatings: Optimization of the manufacturing route and durability under cyclic oxidation, *Thin Solid Films*, DOI 10.1016/j.tsf.2010.08.125.

[8] J. G. Gao, Y. D. He and W. Gao, Synthesis of hollow yttria partially stabilized zirconia (YPSZ) fibers using cotton fibers as template, *Nanoscience and Nanotechnology Lett.* **1** (2009), 1.

[9] C. C. Berndt and J. H. Yi, The Manufacture and microstructure of fiber-reinforced thermally sprayed coatings, *Surf. Coat. Technol.* **37** (1989), 89.

[10] A. P. S. Selvadurai, On the mode I stress intensity factor for an external circular crack with fibre bridging, *Compo. Struct.* **92** (2010), 1512.

[11] J. Aveston and A. Kelly, Theory of multiple fracture of fibrous composites, *J. Mater. Sci.* **8** (1973), 352.

[12] J. Bowling and G. W. Groves, The propagation of cracks in composites consisting of ductile wires in a brittle matrix, *J. Mater. Sci.* **14** (1979), 443.

[13] J. Backlund, Fracture analysis of notched composites, *Comput. Struct.* **13** (1981), 145.

[14] A. P. S. Selvadurai, On three-dimensional fibrous flaws in unidirectional fibre reinforced elastic composites, *Z. Angew. Appl. Math. Phys.* **34** (1983), 51.

[15] L. N. McCartney, Mechanics of matrix cracking in brittle-matrix fibre-reinforced composites, *Proc. Roy. Soc. Ser. A* **409** (1987), 329.

[16] B. Budiansky, J. W. Hutchinson and A. G. Evans, Continuum theory of dilatant transformation toughening in ceramics, *J. Mech. Phys. Solids.* **34** (1986), 167.

[17] D. Chwingel, R. Taylor, T. Haubold, J. Wigren and C. Gualco, Mechanical and thermophysical properties of thick PYSZ thermal barrier coatings: correlation with microstructure and spraying parameters, *Surf. Coat. Technol.* **108** (1998), 99.

[18] D. E. Wolfe, J. Singh, R. A. Miller, J. I. Eldridge and D. M. Zhu, Tailored microstructure of EB-PVD 8YSZ thermal barrier coatings with low thermal conductivity and high thermal reflectivity for turbine applications, *Surf. Coat. Technol.* **190** (2005), 132.